

Electronic structure of La_2CoSi_3 - a non-Kondo analogue of a Kondo lattice, Ce_2CoSi_3

SWAPNIL PATIL, GARIMA SARASWAT, GANESH ADHIKARY, R. BINDU, E. V. SAMPATHKUMARAN AND KALOBARAN MAITI ^(a)

Department of Condensed Matter Physics and Materials' Science, Tata Institute of Fundamental Research, Homi Bhabha Road, Colaba, Mumbai 400005, India

PACS 75.30.Mb – Valence fluctuation, Kondo lattice, and heavy-fermion phenomena
PACS 79.60.Bm – Clean metal, semiconductor, and insulator surfaces
PACS 71.27.+a – Strongly correlated electron systems; heavy fermions

Abstract – We study the electronic structure of a Pauli paramagnetic compound, La_2CoSi_3 using photoemission spectroscopy and *ab initio* band structure calculations. Experimental valence band spectra exhibit signature of electron correlation induced feature around 2.5 eV - the correlation strength among Co 3d electrons is estimated to be close to 3 eV. The Co 2p core level spectra also exhibit correlation induced satellite features consistent with the scenario in the valence band spectra suggesting importance of conduction electron correlation in addition to the local moment in Kondo lattice systems. The La_2CoSi_3 valence band spectra could be utilized to extract Ce 4f related spectral features and thus provide a good reference to study Kondo lattice systems in this class of materials. Temperature evolution of various core level spectra is found to be complex revealing deviations from a typical Fermi liquid behavior and emergence of distinct surface-bulk difference in the electronic structure at finite temperature.

Introduction. – Kondo physics has been one of the most studied subjects in the contemporary condensed matter physics for many decades. [1, 2] A lot of emphasis is given on Ce-based intermetallic compounds for their varied electronic properties such as valence fluctuations, Kondo screening, heavy fermion superconductivity etc. Such properties are known to arise due to the subtle tuning of the hybridization between the Ce 4f electrons and the valence electrons. The theoretical description of such local moment systems is usually captured employing Anderson impurity models. [2, 3] An important input in such descriptions is the correct estimation of the valence band spectral functions for the calculation of the hybridization induced effects. [4–7] There have been efforts to utilize various model spectral functions as an approximation for such a description. In many cases, photon energy dependence of the photoemission cross section of various electronic states has been utilized to experimentally extract Ce 4f related partial density of states. [8]

The electronic structure of a unoccupied 4f homologue of the Ce-based systems can be exploited to extract the parameters more precisely pertinent to the Ce 4f-valence

states hybridization in a realistic scenario. While any of the Ce-based system can be considered for such investigations, we chose here '213' ($R_2\text{CoSi}_3$; R = rare-earths) class of materials, [9] which can be formed easily in single phase, one can continuously tune the electronic properties from Pauli paramagnetic phase to Kondo lattice limit via a single impurity regime. La_2CoSi_3 forms in AlB_2 type hexagonal structure as shown in Fig. 1(a) and 1(b), where La forms hexagonal layers sandwiched by (CoSi_3) layers - top view shown in Fig. 1(b) depicts the atomic arrangements in the layers. Among large number of materials studied in this class, Ce_2CoSi_3 is well established to be a concentrated Kondo lattice system. [10] La substitution in Ce_2CoSi_3 helps to dilute the Ce-density thereby pushing the system towards single impurity regime. It has been observed that strong Kondo coupling strength in this systems necessitates a large degree of substitution ($> 50\%$ of Ce density) to achieve deviation from the typical Kondo lattice behavior. [11] The end member La_2CoSi_3 is a Pauli paramagnetic metal and therefore, an ideal compound to provide a testing ground for the studies of Kondo lattice system in this interesting class of materials.

^(a)Corresponding author: kbmaiti@tifr.res.in

We employed *x*-ray photoemission and ultraviolet pho-

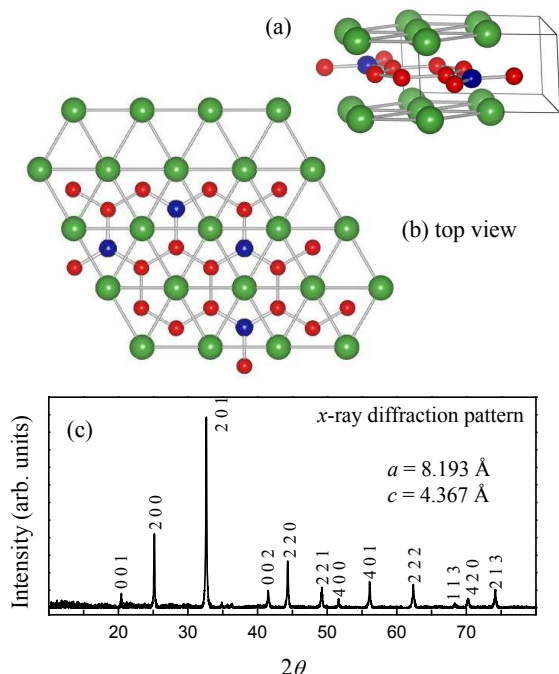


Fig. 1: (a) Crystal structure of La_2CoSi_3 . (b) Top view of the same crystal structure to visualize the atomic arrangements in each layer with clarity. (c) X-ray diffraction pattern of La_2CoSi_3 .

toemission spectroscopy to directly probe the electronic structure and discuss the results in comparison with those for Ce_2CoSi_3 . Our results reveal interesting electronic structure with significant anomaly albeit this compound being Pauli paramagnetic. The comparative study helps to identify effects due to the electron correlation involving Ce $4f$ states distinct from the Fermi liquid behavior. Additionally, the core level spectra show unusual evolution with temperature.

Experimental details. – La_2CoSi_3 was prepared by melting together stoichiometric amounts of high purity (> 99.9%) La, Co and Si in an arc furnace in the atmosphere of high purity argon. The sample was annealed at 750 °C for one week and then characterized by x-ray diffraction (XRD). The XRD pattern, shown in Fig. 1(c), exhibits sharp diffraction peaks corresponding to the AlB_2 -derived hexagonal structure (space group $P6/mmm$) [9] suggesting the sample to be in single phase.

The photoemission measurements were performed using a Gammatdata Scienta R4000 analyzer and monochromatic laboratory photon sources at an energy resolutions set to 0.4 eV and 2 meV at Al $K\alpha$ (1486.6 eV) and He $\text{II}\alpha$ (40.8 eV) photon energies, respectively. The base pressure in the vacuum chamber was 3×10^{-11} Torr. The temperature variation down to 10 K was achieved by an open cycle He cryostat (LT-3M, Advanced Research Systems, USA). The clean surface of the melt grown ingots (extremely hard to cleave) was obtained by *in situ* fracturing and/or scraping - the surface cleanliness was ensured by the absence of

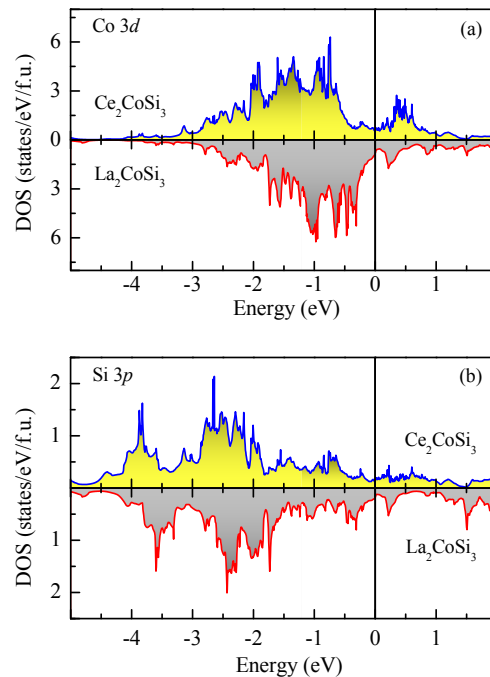


Fig. 2: Calculated (a) Co $3d$ and (b) Si $3p$ partial density of states of Ce_2CoSi_3 and La_2CoSi_3 within local density approximation (LDA).

O $1s$ and C $1s$ features in the x-ray photoelectron spectra and the absence of impurity features in the binding energy range of 5-6 eV in the ultraviolet photoelectron spectra. Both the surface preparation procedures resulted similar data. The reproducibility of the spectra was confirmed after each trial of cleaning process.

The electronic band structures corresponding to the experimentally found ground state were calculated employing *state-of-the-art* full potential linearized augmented plane wave (FLAPW) method using WIEN2k software [12] within the local density approximations, LDA. The convergence for different calculations were achieved considering 512 k points within the first Brillouin zone. The lattice constants used in these calculations are determined from the x-ray diffraction patterns ($a = 8.193$ Å and $c = 4.367$ Å) for La_2CoSi_3 . The lattice constants for Ce_2CoSi_3 were taken from elsewhere. [9]

Results and discussions. – The calculated Co $3d$ and Si $3p$ partial density of states (PDOS) for Ce_2CoSi_3 and La_2CoSi_3 are shown in Fig. 2(a) and 2(b), respectively. The $4f$ PDOS are not shown here as these contributions in La_2CoSi_3 appear in the unoccupied part of the electronic structure. The $4f$ bands in Ce_2CoSi_3 are barely occupied. Therefore, the influences of the $4f$ electrons and the correlations among them are insignificant in the occupied part of the electronic structure in the energy scale shown here. The energy distribution of Co $3d$ and Si $3p$ PDOS for both Ce_2CoSi_3 and La_2CoSi_3 resemble well

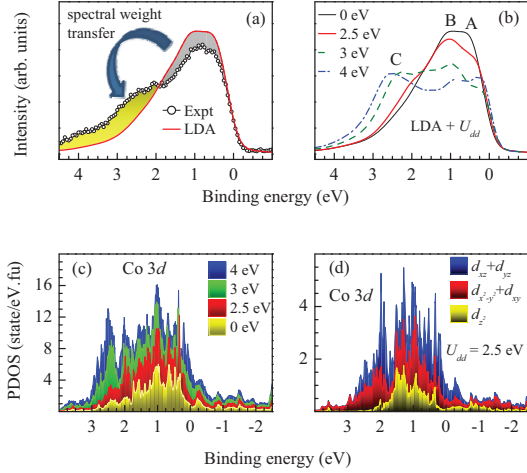


Fig. 3: (a) The experimental x -ray photoemission spectrum (circles) of the valence band spectrum (circles) of La_2CoSi_3 and the spectral function calculated from LDA results (line). (b) Photoemission spectral function for different values of U_{dd} obtained from $\text{LDA} + U_{dd}$ results. (c) Stacked area plot of Co $3d$ PDOS for various values of U_{dd} . (d) Stacked area plot of Co $3d_{z^2}$, $(3d_{x^2-y^2} + 3d_{xy})$ and $(3d_{xz} + 3d_{yz})$ PDOS.

to each other, except there is a rigid energy shift of about 0.35 eV towards lower energies in Ce_2CoSi_3 - this could be attributed to the Fermi level shift arising from larger electron count of Ce. There is a strong mixing of the Co $3d$ and Si $3p$ states. The density of states near the chemical potential are the anti-bonding bands having dominant Co $3d$ character. The bonding bands appear beyond -1.5 eV and possess large Si $3p$ character.

In Fig. 3(a), we compare the calculated results with the experimental valence band spectrum. The integral background subtracted experimental x -ray photoemission (XP) valence band spectrum for La_2CoSi_3 is shown by open circles exhibiting primarily two features centered around 0.5 eV and 2.5 eV binding energies. The theoretical representation of the valence band spectra was simulated as follows. The PDOSs for La $5d$, Co $3d$ and Si $3p$ per formula unit were multiplied by the corresponding photoemission cross-sections for x -ray photoemission spectroscopy using 1486.6 eV photon energy. [13] The results were then convoluted by a Lorentzian function to account for the lifetime broadening and a Gaussian function to account for the instrumental resolution broadening. The calculated spectra are shown by lines in the figure. Evidently, the feature around 0.5 eV is overestimated in the spectral function corresponding to the LDA results and the feature around 2.5 eV marked by '★' in the figure is highly underestimated. Such large difference between the experimental spectrum and the LDA results can be attributed to the correlation induced effect among the Co $3d$ electrons, which are known to be correlated leading to

significant local moment and it is often underestimated in the LDA calculations. Thus, the experimental features at 0.5 eV and 2.5 eV can be termed as coherent and incoherent features, respectively. [14]

In order to capture this scenario of the correlation induced effect in the electronic structure, we have performed $\text{LDA} + U$ calculations for different correlation strength among Co $3d$ electrons, U_{dd} . The simulated valence band spectra for different values of U_{dd} is shown in Fig. 3(b). The shape of the coherent feature is better represented in the $\text{LDA} + U$ data with the two distinctly identifiable features A and B having comparable intensities with the experimental spectrum. An intense feature, C gradually develops with the increase in U_{dd} value. This is evident in the Co $3d$ PDOS shown in Fig. 3(c). Co $3d$ orbital contributions for $U_{dd} = 2.5$ eV are shown in Fig. 3(d) exhibiting weak influence of U_{dd} on the electrons possessing $3d_{z^2}$ character while all others exhibit large spectral weight transfer. The curves corresponding to 2.5 eV and 3 eV in Fig. 3(b) appear to be very similar to the experimental results providing an estimate of the Hubbard, U of about 3 eV. This value is quite similar to the estimations in analogous systems. [15] Further increase in U_{dd} leads to much higher binding energy of the correlation induced feature and a large depletion in intensity around 1 eV.

It is to note here that all the calculated results presented above correspond to the experimentally found ground state of both the materials. It may happen that the approximations in these density functional approaches may lead to a significantly different magnetic ground state as found in a classic case of Pu. [16] In such a case, one needs to consider different calculational method such as $\text{LDA} + \text{DMFT}$ (DMFT = dynamical mean field theory) to capture the experimental scenario. [17] We hope that the results in this study would help to initiate further studies in these directions. Despite simplicity of the method of calculating the electronic structure followed here, the representation of the experimental spectra shown in Fig. 3 is remarkable and suggests a good starting point for the study of these complex systems. Clearly, the heavy Fermion systems with transition metal d electrons as conduction electrons are more complex due to the finite correlation among the conduction electrons.

The above results exemplify the importance of non- f homologue in the study of heavy Fermion physics in $4f$ based compounds. We now investigate the temperature evolution of the valence band spectra of this non-Kondo system in Fig. 4 - the spectra at 10 K and 300 K obtained by x -ray and He II excitations are compared in Fig. 4(a). The two feature structure observed in the XP spectra are also found in the He II spectra at similar energy positions. Relatively sharper lineshape of the near Fermi level feature in the He II spectra appears due to the high energy resolution of the technique. Dominant lifetime broadening at higher binding energies has smeared out the high resolution induced effects in the incoherent feature. The spectra away from the Fermi level exhibit similar lineshape

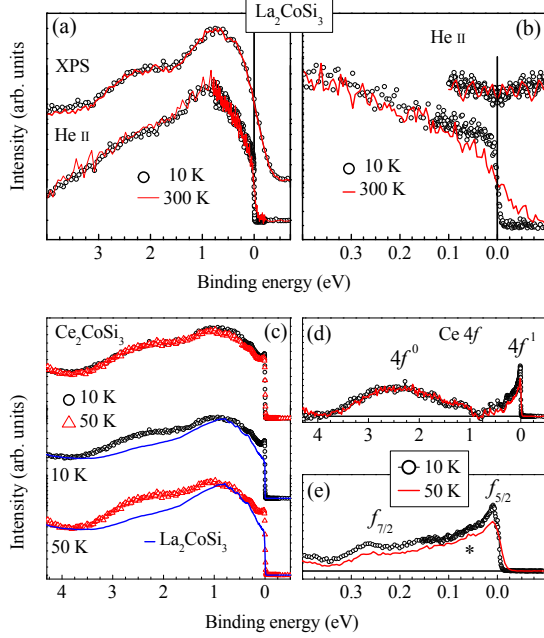


Fig. 4: (a) Valence band spectra of La_2CoSi_3 at 10 K and 300 K obtained by $\text{Al } K\alpha$ and He II excitations. (b) The near Fermi level part of the He II spectra obtained employing high energy resolution is shown here for 10 K and 300 K. The spectral density of states obtained by symmetrization are also shown. (c) He II spectra of Ce_2CoSi_3 at 10 K (circles) and 50 K (triangles) and the corresponding La_2CoSi_3 spectra (lines). (d) Extracted Ce 4f spectral function of Ce_2CoSi_3 at 10 K and 50 K. (e) Expanded near Fermi level part of Ce 4f spectra.

at both the temperatures, 10 K and 300 K.

The features close to the Fermi level in the high resolution He II spectra are shown in Fig. 4(b). The spectra at 10 K and 300 K exhibit normal Fermi liquid type evolution. To verify this behavior further, the near ϵ_F spectra are symmetrized about ϵ_F - such a symmetrized spectral intensity often provides a good representation of the spectral density of states (SDOS) close to ϵ_F . [18] The SDOS for La_2CoSi_3 does not show any change with temperature establishing simple Fermi liquid nature of this material.

These spectral functions can be utilized to extract the Ce 4f contributions from the spectra of a Kondo lattice, Ce_2CoSi_3 having Kondo temperature of about 50 K. [19] In Fig. 4(c), we show the raw data at different temperatures with suitable normalizations to demonstrate the procedure of Ce 4f extraction. The high resolution spectra of La_2CoSi_3 are normalized in such a way that the subtraction of La_2CoSi_3 signal from Ce_2CoSi_3 spectra does not generate unphysical negative intensities. Interestingly, this normalization procedure led to similar background intensities beyond 4 eV. The raw data from Ce_2CoSi_3 at 10 K and 50 K are compared in the upper panel of Fig 4(c) exhibiting temperature dependence as expected due to Kondo type behavior. The subtracted spectra

($I(\text{Ce}_2\text{CoSi}_3) - I(\text{La}_2\text{CoSi}_3)$), shown in Fig. 4(d) exhibit two peak structure, typical of the Ce 4f spectral function from hybridized Ce systems, with one peak close to 2.3 eV binding energy and another peak close to ϵ_F . [20, 21] The feature around 2.3 eV is denoted by $4f^0$ and corresponds to the unscreened 4f photoemission ($|4f^1 \rangle \rightarrow |4f^0 \rangle$ transition). The feature at the Fermi level, termed $4f^1$ signal appears due to $|4f^1 \rangle \rightarrow |4f^1_{\text{c}} \rangle$ transition, where a conduction electron coupled to the 4f states screens the photohole. [15, 22] This coupled state contains the contribution from the Kondo states as evident from the enhancement of intensity with the decrease in temperature.

The near ϵ_F part is shown in an expanded scale in Fig. 4(e). There are two distinct feature in the spectra. The feature close to the Fermi level is denoted by $f_{5/2}$ that corresponds to the total angular momentum of (5/2) for the charge transferred 4f electron. The feature around 280 meV corresponds to the final state angular momentum of (7/2). A small kink around 50 meV is also observed as shown by '*' corresponding to the crystal field split final state of $f_{5/2}$ state. Distinct signatures of the Kondo features appearing due to different final states is remarkable and provides incentive to adopt such procedure to study the electronic structure of Kondo lattice systems. Ce 4f weight has been extracted in the past by using different photon energies for the measurements and exploiting the dependence of photoemission cross section on photon energy. [15, 22] Since the electronic states in the valence band are strongly hybridized, they often exhibit exotic behavior due to their uniqueness different from the pure elemental spin-orbitals. Therefore, finding out correct cross-section of these states is difficult. In the present method, such difficulties can be avoided, although the subtle change in the structural parameters in different compositions can modify the uncorrelated electronic structure. Such changes are very small in the present case and can be neglected within the first approximation.

Since, the photoemission spectroscopy reflects the spectral function corresponding to the final states of the photo-excitation process, the presence and absence of the Kondo feature in the electronic structure can also be manifested in the core level spectra. [15] This has been investigated in Fig. 5, where we show the Co 2p core level spectra of Ce_2CoSi_3 in Fig. 5(a) and La_2CoSi_3 in Fig. 5(b). The experimental spectra exhibit large asymmetry towards higher binding energies. [23] While such asymmetry can be attributed to the low energy excitations across the Fermi level in a metallic system, the observed spectral line-shape cannot be captured by simple asymmetric spectral function as shown in the figure. A broad additional feature needs to be considered in both the cases. The presence of this feature is distinct in the case of La_2CoSi_3 and suggest again the correlated nature of the Co 3d electrons. [24–26]

The decrease in temperature has significant influence in the spectral functions in both the compounds as shown in Fig. 5(c) and 5(d). While the satellite feature appears to be similar at both 10 K and 300 K, the main peak ex-

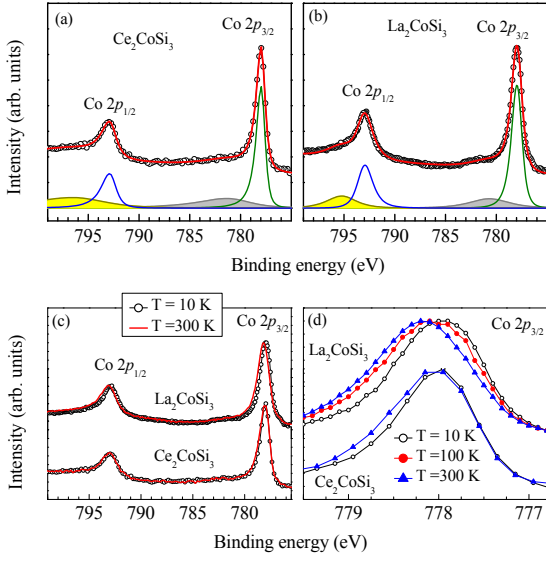


Fig. 5: Co $2p$ core level spectra for (a) Ce_2CoSi_3 and (b) La_2CoSi_3 . The experimental spectra (symbols) are fitted with asymmetric line shapes (lines). The thick solid line superimposed on the symbols are the total fit data. (c) Co $2p$ spectra of Ce_2CoSi_3 and La_2CoSi_3 at 10 K (open circles) and 300 K (lines). (d) Expanded view of the Co $2p_{3/2}$ signal at 10 K (open circles), 100 K (closed circles) and 300 K (triangles).

hibits distinct evolutions. In Ce_2CoSi_3 , the asymmetry of the spectral lineshape is significantly smaller at 10 K than that at 300 K (see Fig. 5(d)). This has been attributed to the formation of Kondo singlets at lower temperatures that leads to larger degree of core hole screening due to the additional f -derived narrow bands near the Fermi level generated by the Kondo coupling. [15] Co $2p_{3/2}$ spectra of La_2CoSi_3 exhibit significantly different temperature evolution - the peak position shifts towards lower binding energies. The lineshape asymmetry seems to increase gradually with the decrease in temperature - the La_2CoSi_3 spectra in Fig. 5(d) exhibit a sharper rise at low temperatures in the low binding energy side with gradual fall in intensity at the other side.

The temperature dependence of La $3d$ core level spectra is plotted in Fig. 6(a) and 6(b). There are two distinct features for each of the spin-orbit split lines - the features marked as $4f^0$ & $4f^1$ appearing around 836 eV & 832.5 eV binding energies for the $3d_{5/2}$ signal, and 852.8 eV & 849.3 eV for the $3d_{3/2}$ signal, respectively correspond to the poorly screened and well screened final states of the $3d$ photoemission. We observe an additional feature about 3.5 eV binding energy higher than the $4f^0$ peak appearing in both $3d_{5/2}$ and $3d_{3/2}$ signals. In order to identify the origin of this feature, we carried out the measurements of $3d$ spectrum at 60° emission angle, which makes the technique significantly surface sensitive. [27] Clearly, the higher binding energy feature enhances in intensity

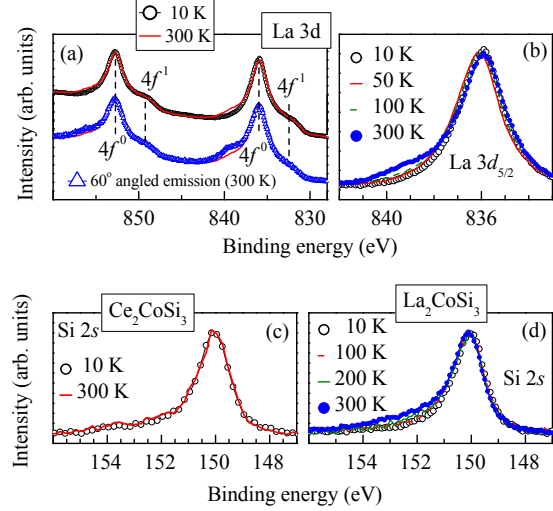


Fig. 6: (a) La $3d$ spectra La_2CoSi_3 collected at 10 K (open circles) & 300 K (line) at normal emission, and the 300 K spectrum collected at 60° angled emission (open triangles). (b) La $3d_{5/2}$ photoemission spectra at 10 K (open circles), 50 K (solid line), 100 K (dashed line) and 300 K (closed circles). (c) Si $2s$ spectra of Ce_2CoSi_3 at 10 K (open circles) and 300 K (solid line). (d) Si $2s$ spectra of La_2CoSi_3 at 10 K (open circles), 50 K (solid line), 100 K (dashed line) and 300 K (closed circles).

with the increase in surface sensitivity indicating its surface character. Decrease in temperature from 300 K to 10 K does not have significant influence in the spectral lineshape corresponding to the bulk electronic structure, while the surface feature appear to decrease gradually with the decrease in temperature (see Fig. 6(b)) and becomes almost non-existent at 10 K. This is a unique behavior of this material exhibiting surface bulk differences in the electronic structure as the temperature is raised, which can have significant implication in device applications.

We investigate the Si $2s$ core level spectra in Fig. 6(c) and 6(d), for Ce_2CoSi_3 and La_2CoSi_3 , respectively. Each of the spectra exhibit sharp single peak structure with large asymmetry towards higher binding energies. The temperature dependence of Si $2s$ core level of Ce_2CoSi_3 shows almost identical lineshape at 10 K and 300 K. A small increase in the Doniach-Šunjić asymmetry at higher binding energies at higher temperatures is observed in the case of La_2CoSi_3 . The change was inferred to be of bulk origin through varying the emission angle of the photoelectrons (not shown here) by 60° as was done above for the La $3d$ core level. The energy shift of the peak position in Si $2s$ and La $3d$ spectra is negligible.

Evidently, the core level spectra of La_2CoSi_3 shows interesting evolution of the lineshape and peak positions with the change in temperature. The decrease in asymmetry with the decrease in temperature can be attributed to the Kondo-resonance behavior due to Fermi surface reconstructions induced by the Kondo singlets at low temperatures. While such an effect is not observed in non-Kondo system, La_2CoSi_3 , this system shows significant anomalies

in all the core levels. Co $2p$ peak shifts and become more asymmetric at lower temperatures. A surface feature disappears in the La $3d$ spectra and the asymmetry in Si $2s$ reduces at low temperatures. All these effects, may be related to the emergence of surface-bulk differences in the electronic structure at higher temperatures, reveals complexity of the problem.

conclusions. – In summary, we studied the electronic structure of La_2CoSi_3 using high resolution photoemission spectroscopy and compared it with the band structure calculations. The valence band spectra of La_2CoSi_3 showed Fermi liquid evolution of the spectral intensity close to ϵ_F . The symmetrized He Π spectra does not show a change in the spectral density of states as a function of temperature in this system. The comparison of the valence band spectra with the simulated ones from the LDA + U results suggests the existence of electron correlations among the Co $3d$ electrons and the corresponding Hubbard, U is close to 3 eV. The Co $2p$ core level spectra exhibit significantly intense satellite features providing further evidence of the correlation induced effects in the electronic structure. We show that the spectral functions of this material can be utilized to extract the Ce $4f$ contributions from the Ce_2CoSi_3 spectra. Comparison of the temperature evolution of Co $2p$ lineshape is found to be different in Kondo and non-Kondo systems, which may be utilized as a signature of Kondo behavior. The La $3d$ core spectra reveal a surface feature as the temperature is raised suggesting emergence of surface-bulk differences at finite temperatures. The Co $2p$ and Si $2s$ peaks exhibit curious evolution with temperature. The anomalies in the core level spectra may have relation to the emergence of the surface-bulk differences at higher temperatures.

Acknowledgements. – The author, S. P. thanks the Council of Scientific and Industrial Research, Government of India for financial support. All the authors thank Mr. Kartik K. Iyer for his help in sample preparation and characterization.

REFERENCES

- [1] Brandt N. B. and Moshchalkov V. V., *Advances in Physics* **33** (1984) 373.
- [2] Bulla R., Costi T. and Pruschke T., *Rev. Mod. Phys.* **80**, (2008) 395; Benlagra A., Pruschke T. and Vojta M., *Phys. Rev. B* **84** (2011) 195141; Prüser H. *et al.*, *Nature Physics* **7** (2011) 203.
- [3] Anderson P. W., *Phys. Rev.* **124** (1961) 41.
- [4] Wills J. M. and Cooper B. R., *Phys. Rev. B* **36** (1987) 3809.
- [5] Gunnarsson O. and Jepsen O., *Phys. Rev. B* **38** (1988) 3568.
- [6] Gunnarsson O., Andersen O. K., Jepsen O. and Zaanen J., *Phys. Rev. B* **39** (1989) 1708.
- [7] Gunnarsson O. and Schönhammer K., *Phys. Rev. B* **40** (1989) 4160.
- [8] Andrews A. B. *et al.*, *Phys. Rev. B* **53** (1996) 3317.
- [9] Gordon R. A. *et al.*, *J. Alloys Compounds* **248** (1997) 24.
- [10] Chevalier B. *et al.*, *Solid State Commun.* **49** (1984) 753; Das I. and Sampathkumaran E. V., *J. Magn. Magn. Mater.* **137** (1994) L239; Mallik R. *et al.*, *J. Magn. Magn. Mater.* **185** (1998) L135.
- [11] Majumdar S. *et al.*, *Physica B* **281&282** (2000) 367; *ibid.*, *Solid State Commun.* **110** (1999) 509.
- [12] P. Blaha, K. Schwarz, G. K. H. Madsen, D. Kvasnicka, and J. Luitz, **WIEN2k**, An Augmented Plane Wave + Local Orbitals Program for Calculating Crystal Properties (Karlheinz Schwarz, Techn. Universität Wien, Austria), 2001. ISBN 3-9501031-1-2.
- [13] Yeh J. J. and Lindau I., *At. Data Nucl. Data Tables* **32** (1985) 1.
- [14] Fujimori A. *et al.*, *Phys. Rev. Letts.* **69** (1992) 1796; Inoue I. H. *et al.*, *Phys. Rev. Letts.*, **74** (1995) 2539; Maiti K., Mahadevan P. and Sarma D. D., *Phys. Rev. Letts.* **80** (1998) 2885.
- [15] Patil S. *et al.*, *J. Phys.: Condens. Matter* **22** (2010) 255602; Patil S. *et al.*, *Phys. Rev. B* **82** (2010) 104428; Patil S. *et al.*, *Europhys. Letts.* **97** (2012) 17004.
- [16] Savrasov S. Y., Kotliar G. and Abrahams E., *Nature* **410** (2001) 793; Savrasov S. Y. and Kotliar G., *Phys. Rev. Letts.* **84** (2000) 3670.
- [17] Jarrell M. and Pruschke T., *Phys. Rev. B* **49** (1994) 1458; Cox D. L. *et al.*, *Europhys. Letts.* **21** (1993) 593; Pruschke T., Cox D. L. and Jarrell M., *Phys. Rev. B* **47** (1993) 3553; Singh R. S. *et al.*, *Phys. Rev. B* **77** (2008) 201102; Georges A. *et al.*, *Rev. Mod. Phys.* **68** (1996) 13.
- [18] Medicherla V. R. R. *et al.*, *Appl. Phys. Letts.* **90** (2007) 062507.
- [19] Patil S., Iyer K. K., Maiti K. and Sampathkumaran E. V., *Phys. Rev. B* **77** (2008) 094443.
- [20] Gunnarsson O. *et al.*, *Phys. Rev. B* **28** (1983) 7330.
- [21] Allen J. W., Oh S. -J., Maple M. B. and Torikachvili M. S., *Phys. Rev. B* **28** (1983) 5347.
- [22] Ehm D. *et al.*, *Phys. Rev. B* **76** (2007) 045117.
- [23] Doniach S., and Šunjić M., *J. Phys. C: Solid State Phys.* **3** (1970) 285.
- [24] Imada M., Fujimori A. and Tokura Y., *Rev. Mod. Phys.* **70** (1998) 1039; Maiti K., Mahadevan P., and Sarma D. D., *Phys. Rev. B* **59** (1999) 12457.
- [25] Pandey S. K. *et al.*, *Phys. Rev. B* **77** (2008) 115137; Pandey S. K. *et al.*, *Phys. Rev. B* **77** (2008) 045123.
- [26] Schneider C. M., *Phys. Rev. B* **54** (1996) R15618.
- [27] Maiti K. *et al.*, *Phys. Rev. B* **73** (2006) 052508.